Short-term variability of overcast brightness

Raymond L. Lee, Jr. and Javier Hernández-Andrés

Overcasts seen from below seldom are uniform, unchanging cloud shields, yet little is known about their short-term photometric variability (periods ≤2 h). Visible-wavelength spectra of daytime and twilight overcast skies measured at 30-s intervals reveal unexpected temporal variability in horizontal illuminance E_v and zenith luminance L_v. Fourier analysis of these time series shows peak fluctuations at periods of 2–40 min. Factors such as cloud type and optical depth, presence of fog or snow, and instrument field of view can affect overcast brightness variability. Surprisingly, under some circumstances overcast twilight E_v exceeds clear-sky E_v at the same Sun elevation.

OCIS codes: 010.1290, 290.1090, 290.4210, 290.7050.

1. Introduction

To casual observers at the Earth's surface, the overcast sky may seem to be the epitome of visual monotony, a nearly featureless shield of gray cloud. Yet overcasts' transmission of daylight is seldom gray or spectrally neutral,[1] and most stratocumulus overcasts have myriad luminance details that quickly move and change shape (see Fig. 1). Even seemingly uniform stratus overcasts can exhibit pronounced illuminance changes from minute to minute, a fact long recognized by lighting engineers.[2,3] More recently, researchers analyzing climate and radiative transfer models have emphasized that these models must include small-scale spatial and temporal fluctuations in overcast optical depth and transmitted irradiance.[4–8]

Yet despite this recent work on overcasts' radiometric variability, we have found no comparable research that examines their photometric variability as measured from below. In particular, we are interested in analyzing short-term fluctuations in overcast horizontal illuminance and zenith luminance as measured every 30 seconds for total elapsed times $t_{el} \leq 2$ h. Our choice of sampling frequency and maximum measurement period reflects constraints imposed by (1) our spectroradiometers' long integration times at twilight illuminance levels and (2) measurement interruptions due to the onset of rain or clearing in some overcasts. Although our chosen sampling frequency would be too low to capture all photometric details of the most rapidly changing partly cloudy skies,[9] for many overcasts it is more than adequate to reveal a remarkable range of illuminance and luminance fluctuations.

2. Measuring Overcast Horizontal Illuminances and Zenith Luminances

Consistent with our earlier definition of "overcast," we analyze brightness fluctuations only in those skies with complete cloud coverage.[10] We calculate overcast horizontal illuminances E_v and zenith luminances L_v from our earlier time series of >9100 irradiance and radiance spectra measured during 40 different overcasts; integrals are calculated from 380–780 nm in 4 nm steps. Our observing sites are the U.S. Naval Academy (USNA) at Annapolis, Maryland, the University of Granada at Granada, Spain, and two rural sites near Owings, Maryland and Marion Center, Pennsylvania. See Ref. 1, Sect. 2 for other details of our sites and spectroradiometers.

Figure 2 suggests the wide range of short-term variability in our overcast E_v time series. In it we show E_v as a function of unrefracted Sun elevation h_0 for two USNA stratus overcasts on 11-21-02 and 10-17-03. We use h_0 as Fig. 2's abscissa because for a given overcast optical depth τ, overcast E_v at the surface depends on downwelling irradiance atop the clouds, which itself is largely determined by h_0. Because we acquired data after solar noon on most days, we make h_0 decrease and time increase from left to right in Fig. 2 and later figures. For brevity, we use

R. L. Lee (raylee@usna.edu) is with the Mathematics and Science Division, United States Naval Academy, Annapolis, Maryland 21402. J. Hernández-Andrés is with Departamento de Óptica, Facultad de Ciencias, Universidad de Granada, Granada 18071, Spain.

Received 23 December 2004; revised manuscript received 15 April 2005; accepted 3 May 2005.

0003-6935/05/275704-08$15.00/0

Report Documentation Page

Form Approved
OMB No. 0704-0188

1. REPORT DATE	2. REPORT TYPE	3. DATES COVERED
15 APR 2005		**00-00-2005 to 00-00-2005**

4. TITLE AND SUBTITLE	5a. CONTRACT NUMBER
Short-term variability of overcast brightness	5b. GRANT NUMBER
	5c. PROGRAM ELEMENT NUMBER
6. AUTHOR(S)	5d. PROJECT NUMBER
	5e. TASK NUMBER
	5f. WORK UNIT NUMBER
7. PERFORMING ORGANIZATION NAME(S) AND ADDRESS(ES) **United States Naval Academy (USNA),Mathematics & Science Department,Annapolis,MD,21402**	8. PERFORMING ORGANIZATION REPORT NUMBER
9. SPONSORING/MONITORING AGENCY NAME(S) AND ADDRESS(ES)	10. SPONSOR/MONITOR'S ACRONYM(S)
	11. SPONSOR/MONITOR'S REPORT NUMBER(S)

12. DISTRIBUTION/AVAILABILITY STATEMENT
Approved for public release; distribution unlimited

13. SUPPLEMENTARY NOTES

14. ABSTRACT

15. SUBJECT TERMS

16. SECURITY CLASSIFICATION OF:			17. LIMITATION OF ABSTRACT	18. NUMBER OF PAGES	19a. NAME OF RESPONSIBLE PERSON
a. REPORT **unclassified**	b. ABSTRACT **unclassified**	c. THIS PAGE **unclassified**	**Same as Report (SAR)**	**8**	

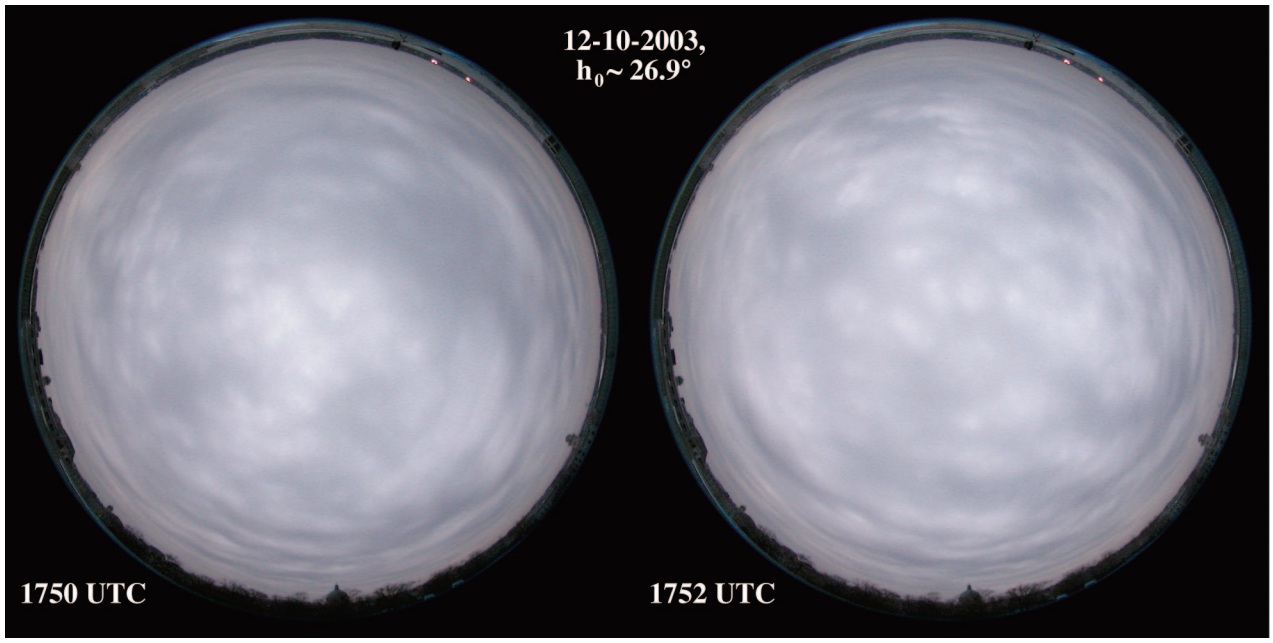

Fig. 1. Fisheye photographs of a rapidly changing stratocumulus overcast taken at 1750 and 1752 UTC on 12-10-2003 at the U.S. Naval Academy in Annapolis, Maryland (USNA). Nikon E5000 digital camera shutter speeds are 1/215 s on the left and 1/190 s on the right; white balance and other exposure parameters (ISO 100 equivalent sensitivity, $f/5.0$ aperture) are the same in both photographs. Light rain began falling soon afterward at ~1810 UTC.

conventional meteorological abbreviations in these figures: "OVC" for overcast, "CLR" for clear, "St" for stratus, and "Sc" for stratocumulus.

Not surprisingly, the overcast E_v in Fig. 2 are much smaller than those for the 9-10-03 clear sky. In particular, mean E_v on the two overcast afternoons is ~3.1 times smaller than mean clear-sky E_v for $27.1° > h_0 > 21.6°$. Although there are important exceptions (see Sect. 5), the common observation that horizontal illuminance is less beneath overcasts than clear skies at the same h_0 is a long-lived truism in atmospheric optics.[11] Bohren succinctly explains this commonplace within the confines of a two-stream model of scattering and absorption by optically thick clouds.[12]

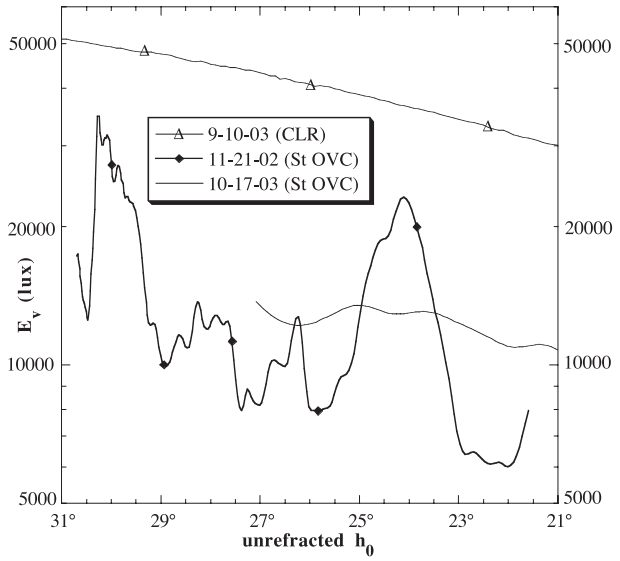

Fig. 2. Spectrally integrated horizontal illuminance E_v as a function of unrefracted Sun elevation h_0 for parts of one clear and two overcast afternoons at USNA. Note that E_v is scaled logarithmically.

Although Fig. 2's two overcasts have similar mean E_v, their temporal details differ greatly. For example, E_v from the much more variable 11-21-02 overcast decreased 74% in one 19-min period ($24.1° > h_0 > 22.0°$), whereas E_v decreased only ~15% on 10-17-03 during the same h_0 interval (clear-sky E_v decreased 12%). Yet we saw few visual differences between the two stratus overcasts: our field notes for 11-21-02 note an overcast of "varying thickness with some internal structure," while that on 10-17-03 was simply "fairly uniform." Neither overcast produced any precipitation at the surface.

Beyond merely computing ratios of consecutive illuminance maxima and minima, how can we quantify E_v temporal variability? One potentially useful metric for comparing the 11-21-02 and 10-17-03 overcasts is D_6, the root-mean-square difference between any given E_v curve and a 6th-order best-fit polynomial P_6 to some smooth E_v curve (in Fig. 3, the smoother 10-17-03 E_v).[13] To determine P_6, we start by normalizing the 11-21-02 curve so that it has the same mean E_v as the 10-17-03 curve on the interval $27.0° > h_0 > 21.5°$. Although this normalization helps reduce D_6 for the slightly darker 11-21-02 overcast, its D_6 of 6424 lux is nonetheless 36.7 times greater than that for 10-17-03 ($D_6 = 175$ lux). Remarkably, such large differences in E_v fluctuations may go unnoticed by *in situ* observers because overcast E_v often change over periods of minutes rather than seconds.

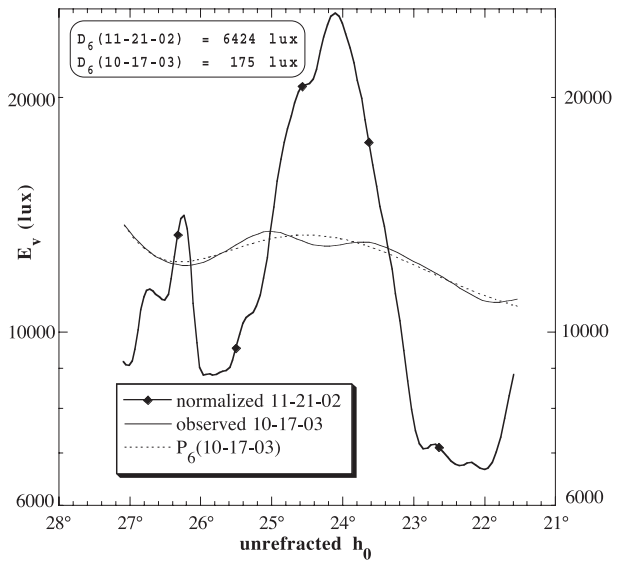

Fig. 3. Portion of Fig. 2's overcast time series with a 6th-order polynomial P_6 (dashed curve) fitted to the smoother 10-17-03 E_v curve. The root-mean-square difference D_6 between P_6 and the observed E_v curves is 36.7 times greater on 11-21-02 than on 10-17-03.

In Fig. 3, h_0 decreases faster on 10-17-03 (t_{el} = 35.5 min) than on 11-21-02 (t_{el} = 54.5 min; see Table 1 for more details). If Fig. 3's abscissa were t_{el} rather than h_0, the 10-17-03 time series' few undulations would be compressed into a shorter distance, and thus would appear somewhat noisier. However, P_6 and D_6 change only slightly if we switch to equal 54.5 min t_{el} that start at $h_0 = 27.0°$ on both days: in that case, D_6(10-17-03) = 196 lux and D_6(11-21-02) = 5372 lux, or the 11-21-02 fluctuations are now 27.4 times greater. Thus the 11-21-02 overcast is much more variable whether our comparison uses h_0 or t_{el}. In fact, we have determined that using h_0 rather than t_{el} to plot overcast time series does not affect any of our qualitative conclusions here.

3. Fourier Analysis of Overcast Brightness Variability

An obvious weakness in Fig. 3's approach to quantifying overcast variability is that it does not preserve any temporal information about E_v fluctuations. Furthermore, we may want to compare overcasts with fluctuations that appear similar in magnitude but dissimilar in temporal frequency. Fourier analysis such as Fig. 4's spectral density function[14] (SDF) lets us quantify overcast variability even if neither E_v curve is sufficiently smooth to determine a meaningful P_6. Note that hereinafter "spectral" means the *temporal* frequency of illuminance or luminance fluctuations in a time series, not the electromagnetic frequencies in a single irradiance or radiance spectrum. SDFs for Fig. 2's overcasts reveal some subtle, but telling, differences between them.

In Fig. 4, the influence of any period Δt on the E_v curve's shape increases with SDF, which itself is proportional to the variance σ^2 of E_v at the given Δt (i.e., SDF(Δt) $\propto \sigma^2(E_v(\Delta t))$). Note that Fig. 4's ordinate is SDF in decibels or 10 $\log_{10}$(SDF). In calculating SDF(Δt), we first subtract the mean E_v or L_v from each time series, so the zero-frequency spectral density (or mean power) is not shown in Fig. 4 and later SDFs.

We start by considering in Fig. 4 the SDF for Fig. 2's least complicated time series, the monotonically decreasing clear-sky E_v of 9-10-03. This SDF is approximately linear, which is consistent with Fig. 2's nearly linear decrease in clear-sky $E_v(h_0)$ for $27.1° > h_0 > 21.5°$.[15] We say it is consistent because a linear function such as Fig. 2's clear-sky $E_v(h_0)$ can be approximated as the sum of sine terms whose coefficients steadily decrease with increasing frequency (or decreasing period). Thus we see a nearly linear power spectrum in Fig. 4 for the 9-10-03 clear-sky E_v. Conversely, departures from linearity in a SDF (e.g., local maxima and minima) indicate that E_v or L_v fluctuations exist at the particular Δt.

How then do we interpret Fig. 4's overcast SDFs? Because the overcast E_v in Fig. 2 are less than the clear-sky E_v, the overcast SDFs' magnitudes are usually smaller. This happens because reducing a time series' mean E_v tends to reduce the magnitudes of its variances and thus its SDF(Δt). However, the *shapes* of Fig. 4's SDF(Δt) curves (as opposed to their magnitudes) are unaffected by a time series' mean E_v. As noted above, local maxima and minima in Fig. 4's

Table 1. Sun-Elevation and Elapsed-Time Intervals for Overcasts

Figure	Date	E_v or L_v[a]	h_0 Interval (°)[b]	t_{el}(min)[b]
2	11-21-02	E_v	30.7–21.6	120.5
2	9-10-03	E_v	31.0–21.0	53.5
2	10-17-03	E_v	27.1–21.0	39.0
3	11-21-02	E_v	27.1–21.6	54.5
3	10-17-03	E_v	27.1–21.5	35.5
5	2-27-03	L_v	37.8–21.0	120.5
5	3-1-03	L_v	38.0–21.1	118.0
7	2-1-03	L_v	30.9–20.0	97.5
7	2-27-03	L_v	35.0–21.0	95.5
9	1-1-03	L_v	25.4–20.0	59.0
9	2-27-03	L_v	26.0–21.0	31.0
10	1-16-03	L_v	19.0–12.0	50.5
10	3-30-03	L_v	18.7–12.3	33.2
11	9-27-02	E_v	18.3–29.3	61.9
11	10-12-03	E_v	22.7–18.6	25.3
11	10-17-03	E_v	27.1–18.0	56.5
11	12-10-03	E_v	28.1–26.4	52.0
12	9-17-98	E_v	4.9–(−5.5)	53.5
12	10-9-98	E_v	4.9–(−6.0)	56.5
12	10-12-02	E_v	12.0–(−5.8)	96.5
13	10-10-99	E_v	5.1–(−4.8)	53.0
13	10-12-02	E_v	6.0–(−5.8)	63.0
13	11-22-03	E_v	6.0–(−5.0)	62.0
14	4-21-03	E_v	30.1–45.0	80.5

[a]Denotes whether the given figure plots illuminance E_v or luminance L_v.

[b]For the given figure, h_0 interval and elapsed time t_{el} indicate the period over which E_v or L_v is plotted. Other figures may show a slightly different t_{el} or h_0 interval from the same day. Morning observations list the smaller h_0 value first, and numbers in parentheses denote $h_0 < 0°$.

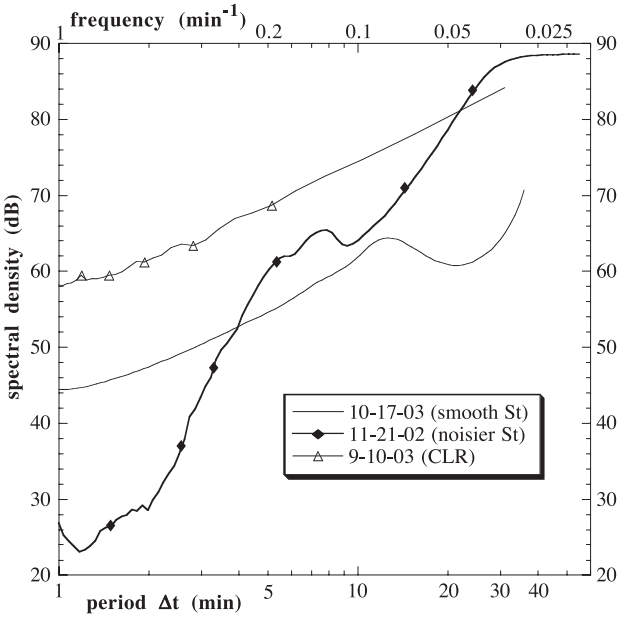

Fig. 4. Power spectra of clear-sky and stratus overcast E_v at USNA (see Fig. 2) as functions of period Δt or temporal frequency $1/\Delta t$ on the interval $27.1° > h_0 > 21.5°$. The spectral density function SDF is defined by Eq. 206c in Ref. 14, and $\mathrm{SDF}(\Delta t) \propto \sigma^2(E_v(\Delta t))$ for variance σ^2. SDF values are given in dB ($10 \log_{10}(\mathrm{SDF})$), and Δt is scaled logarithmically to show more detail at smaller periods.

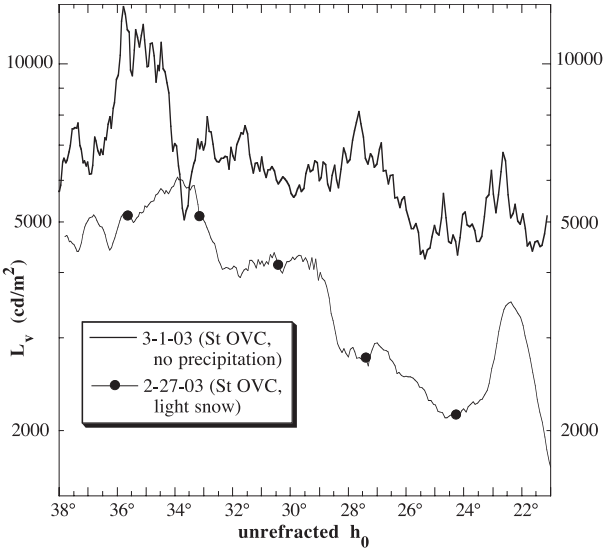

Fig. 5. Spectrally integrated zenith luminance L_v as a function of h_0 for stratus overcasts at Owings, Maryland on the afternoons of 2-27-03 and 3-1-03. On 2-27-03, light snow began falling at the surface when $h_0 \sim 35.7°$, and both the snowfall rate and snowflake size increased slightly during measurements. Note that L_v is scaled logarithmically.

overcast SDFs are caused by E_v fluctuations in the corresponding time series. First, note that because the 10-17-03 SDF has less spectral detail than the 11-21-02 SDF for $\Delta t < 10$ min, the 10-17-03 E_v vary less at high frequencies. Second, the dB range of a SDF curve at low frequencies (here, $\Delta t > 10$ min) indicates the dynamic range or ratio of maximum to minimum E_v in the original time series. Because the 10-17-03 overcast's E_v dynamic range is less than that for 11-21-02 (see Fig. 3), its low-frequency SDF range is also smaller. Third, note the sparse spectral detail in the 11-21-02 SDF for $\Delta t < 5$ min. This means that the 11-21-02 E_v fluctuations with $\Delta t = 5$–30 min do not themselves display much higher-frequency noise.

Not surprisingly, overcast luminances L_v tend to be noisier than E_v because L_v is averaged across a much smaller field of view (FOV): 1° diameter or $\sim 2.4 \times 10^{-4}$ sr in our radiometers, compared with their 2π sr FOV for E_v.[16] Figure 5 shows some of this extra noise associated with L_v's narrower FOV. We may also be tempted to infer from Fig. 5 that thinner, brighter overcasts are noisier than thicker, darker ones: in the thinner overcasts, the same change in cloud thickness Δz should cause a proportionally larger change in cloud transmissivity T.[12]

That seems to be true in Fig. 5, where a brighter, precipitation-free stratus overcast at Owings is consistently more variable than a darker, snowing one. But the appearance of such time series can be deceiving. Figure 6's SDFs for these two skies show that their quite real differences in temporal L_v variability are less than we might think based solely on the time series. Although the 3-1-03 overcast is usually brighter than the 2-27-03 overcast (i.e., its Fig. 6 SDF is larger), the two SDFs are nearly congruent except at the largest and smallest Δt. How do we interpret this fact? Since the SDFs diverge for $\Delta t \sim 2$–7 min and the 3-1-03 SDF has slightly more spectral detail, the "extra" L_v variance appears as high-frequency noise in the 3-1-03 time series. Because the SDFs

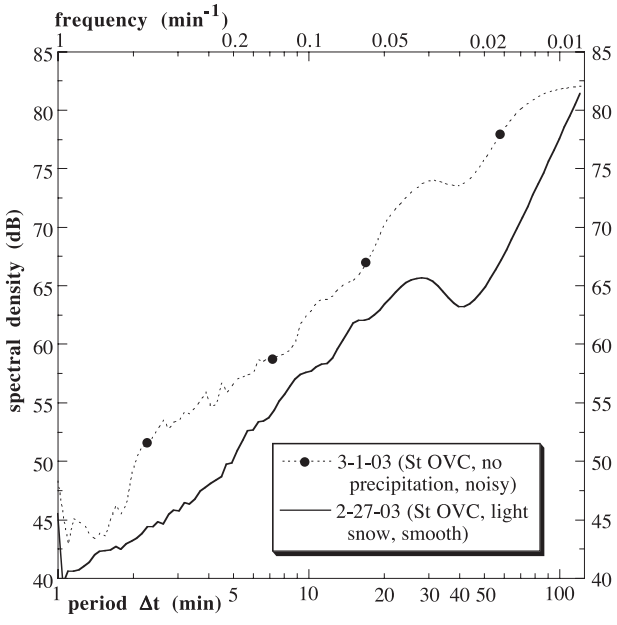

Fig. 6. Power spectra (SDF) of stratus overcast L_v as functions of period Δt or temporal frequency $1/\Delta t$ at Owings on 2-27-03 and 3-1-03 (see Fig. 5 for corresponding L_v time series).

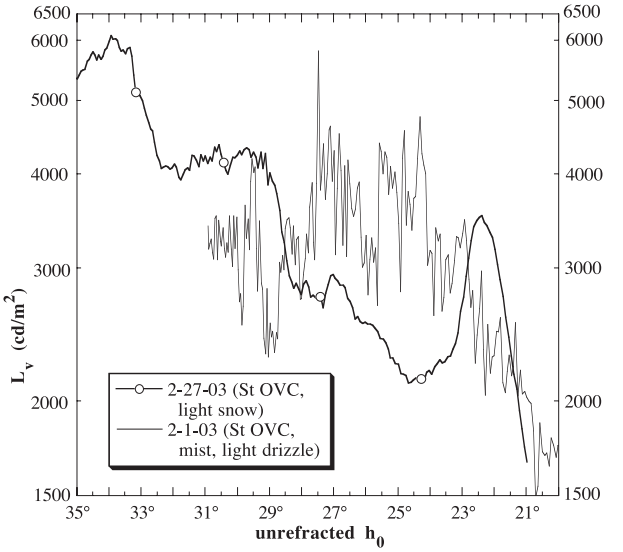

Fig. 7. Zenith L_v as a function of h_0 for stratus overcasts at Owings on the afternoons of 2-1-03 and 2-27-03. Mist and light drizzle accompanied the 2-1-03 overcast, and it has more luminance noise than the snowy 2-27-03 overcast.

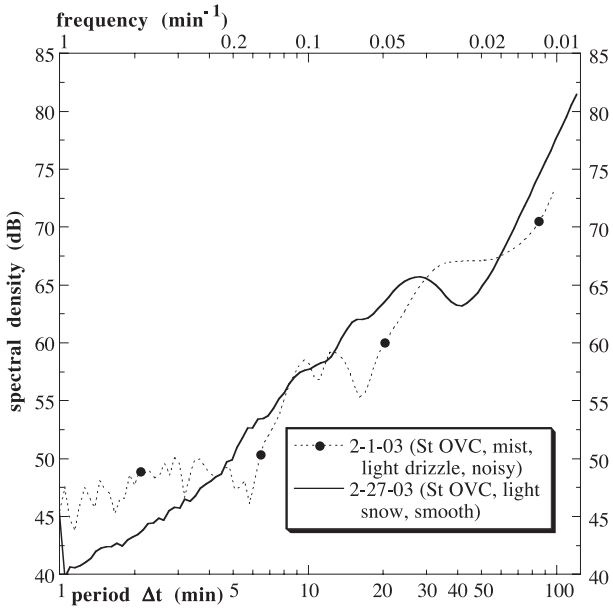

Fig. 8. Power spectra (SDF) of stratus overcast L_v as functions of period Δt or temporal frequency $1/\Delta t$ at Owings on 2-1-03 and 2-27-03 (see Fig. 7 for corresponding L_v time series).

converge for $\Delta t > 40$ min, the time series' variations grow more alike at lower temporal frequencies. For $\Delta t = 10$–30 min, the nearly congruent SDFs mean that both time series have midfrequency waves of similar shape.

Figure 7 offers a clear counterexample to our plausible idea that thicker overcasts are less variable. Here we compare Fig. 5's snowy stratus of 2-27-03 with a drizzling stratus of 2-1-03 at Owings. The latter overcast is both (1) consistently much noisier and (2) alternately darker (thicker) *and* brighter (thinner) than the snowy overcast. Perhaps short-term variability depends on more than total cloud τ: might multiple scattering by snowflakes below the cloud base give a snowing overcast smaller L_v variations than a raining (or precipitation-free) overcast? Figure 7 suggests that this idea is plausible.

Figure 8's SDFs for the Fig. 7 time series clearly show the high-frequency noise on 2-1-03 for $\Delta t < 5$ min. Unlike in Fig. 6, at larger Δt the two Fig. 8 SDFs have no matching maxima or minima, and this accounts for the quite different appearance of the two time series. With some scrutiny, we can just divine in Fig. 7's quite noisy 2-1-03 time series the longer-period fluctuations diagnosed by its SDF local maxima at $\Delta t = 10$–12 min and $\Delta t \sim 35$–40 min. Yet for the smoother 2-27-03 time series, the lowest-frequency local maximum in Fig. 8 is $\Delta t \sim 30$ min. Thus Fig. 7's 2-1-03 time series illustrates a more general point: high-frequency L_v noise may be superimposed on a sky that would otherwise be *less* variable than overcasts lacking such noise.

4. Some Physical Explanations of Overcast Variability

Like Fig. 7, Fig. 9 also shows that a darker, optically thicker overcast (1-1-03 stratus with fog) is not necessarily less variable than a brighter, optically thinner one (2-27-03 snowing stratus). In fact, noisiness differences persist even for the largest L_v difference on the two days (see Fig. 9 at $h_0 \sim 22°$). Puzzling too is the fact that a fog capable of obscuring the cloud base,[17] surely a multiple scattering medium, is noisier than *another* presumably multiple-scattering sub-cloud medium, the light snow falling from the 2-27-03 overcast.

Yet Fig. 10 shows that snow may have no consistent effect on L_v variability. Here a nearly visually featureless stratus overcast on 1-16-03 is consistently

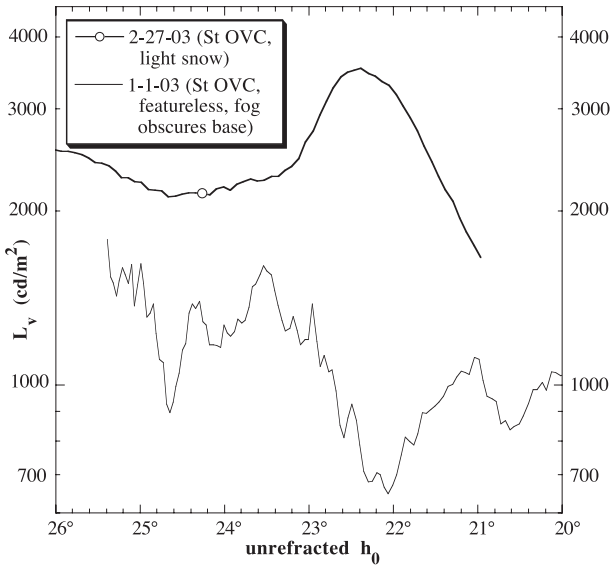

Fig. 9. Zenith L_v as a function of h_0 for stratus overcasts at Owings on the afternoons of 1-1-03 and 2-27-03. Although the darker 1-1-03 overcast looked nearly featureless and had fog below its base, it also has more luminance noise.

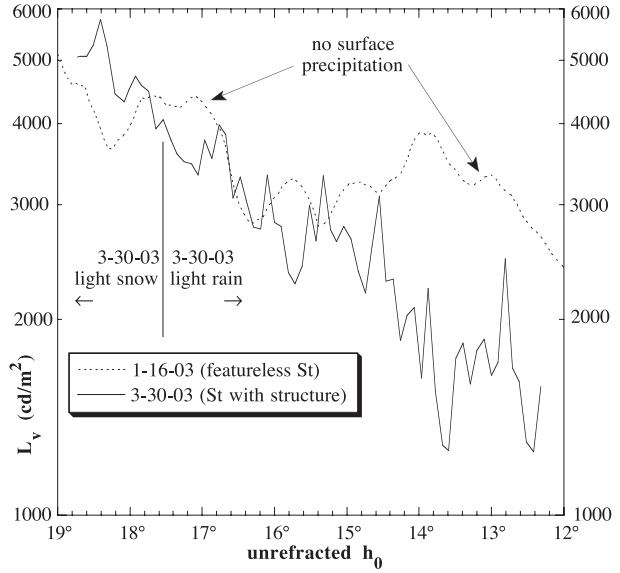

Fig. 10. Zenith L_v as a function of h_0 for stratus overcasts at Owings on the afternoons of 1-16-03 and 3-30-03. Note that luminance noise on 3-30-03 changes little when precipitation changes from light snow to light rain.

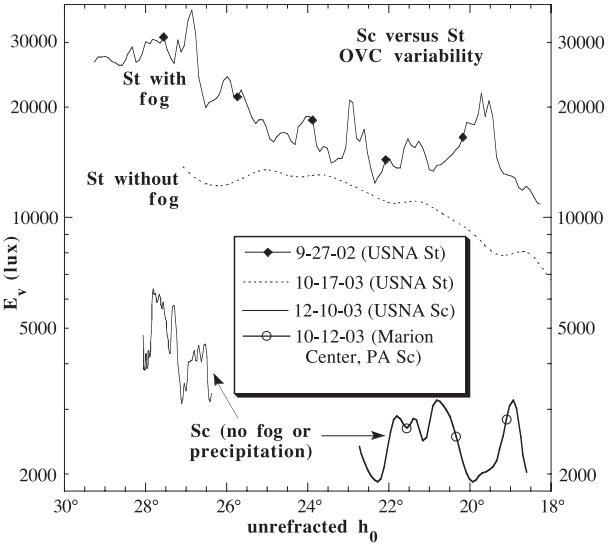

Fig. 11. Horizontal illuminance E_v as a function of h_0 for several stratus and stratocumulus overcasts at USNA (9-27-02, 10-17-03, and 12-10-03) and at a rural site near Marion Center, Pennsylvania (10-12-03).

less noisy than a precipitating one on 3-30-03. Furthermore, mean overcast τ is similar on both dates, and there is no obvious change in the 3-30-03 time series' noisiness when light snow changes to light rain at $h_0 \sim 17.5°$. A more obvious candidate for explaining this noisiness is the clearly visible cloud structure on the latter date.

Does cloud type (e.g., stratus or stratocumulus) affect L_v and E_v variability? Clearly the much greater spatial detail of a stratocumulus overcast can cause rapid L_v fluctuations as cloud features of various τ quickly pass across a radiometer's narrow FOV. Less obvious is how such small-scale features influence E_v variability, for which the radiometer FOV $= 2\pi$ sr. Our data suggest that stratocumulus E_v fluctuations exceed those for stratus at the same h_0 and cloud τ. But since these conditions are rarely met in nature, we can examine only roughly comparable cases.

Figure 11 gives four such cases, and in them overcast variability increases with the presence of fog and/or decreasing cloud τ. In our experience, stratocumulus are often darker and thicker than stratus, and so this partly offsets the former's greater spatial detail. Ultimately, an overcast's temporal variability seems to depend on (and vary directly with) its spatial variability. Perhaps surprisingly, fog usually *increases* overcast variability, perhaps because its subcloud vertical τ fluctuates faster than does cloud τ itself (assuming that the fog is distinguishable from higher-altitude clouds). Alternatively, fog may increase overcast brightness noise simply because fog is closer to the radiometer than clouds and thus fog features' *angular* (as opposed to linear) speed across the radiometer FOV is much greater. This greater angular speed is significant because for zenith angle θ, the $L_v(\theta)$ contributions to horizontal $E_v \propto \cos(\theta)$. Thus even a cosine-corrected diffuser will transmit changes in the angular distribution of radiances above it.

More compellingly, time-lapse photographs taken during our measurements show that fluctuations in overcast L_v and E_v often are caused by cloud elements of different τ that are advected across the radiometer FOV rather than by τ changes occurring within individual elements. Although τ certainly changes in these elements as they move, nonetheless we can often associate local maxima and minima in L_v or E_v with the passage overhead of distinct bright or dark regions in the overcast. The period of these extrema is $\Delta t <$ 10–15 min, so we classify them as mid- to high-frequency fluctuations. However, the presence of small, low-frequency E_v fluctuations in seemingly featureless stratus overcasts (e.g., 10-17-03 case in Figs. 3, 4, and 11) indicates that slow changes in mean overcast τ also contribute to overcast variability.

5. Illuminance Variability during Overcast Twilights

Still another plausible idea is that overcast variability will decrease during evening civil twilight because cloud-top illumination changes from diffuse skylight plus direct sunlight to skylight alone. Twilight's nearly diffuse lighting will reduce E_v differences between lighted and shaded areas on the overcast's top, which in turn might reduce E_v fluctuations beneath the overcast. Of course, as the Sun nears the horizon, we might expect the ever-larger shadows cast by nearby clouds to briefly *increase* E_v variability. Whatever the merits of this logic, Fig. 12 shows that it cannot explain all overcast twilights. Although overcast E_v fluctuations sometimes decrease after sunset (the 10-12-02 case), they also can either persist throughout much of civil twilight (the 10-9-98 case) or scarcely exist before sunset to begin with (the 9-17-98

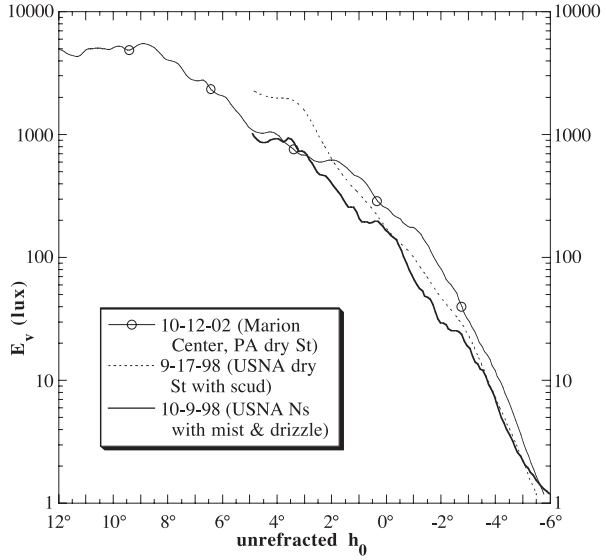

Fig. 12. Horizontal illuminance E_v as a function of h_0 before and during three overcast twilights at Marion Center (10-12-02) and USNA (9-17-98 and 10-9-98). Nimbostratus (Ns) comprised the base of the 10-9-98 overcast.

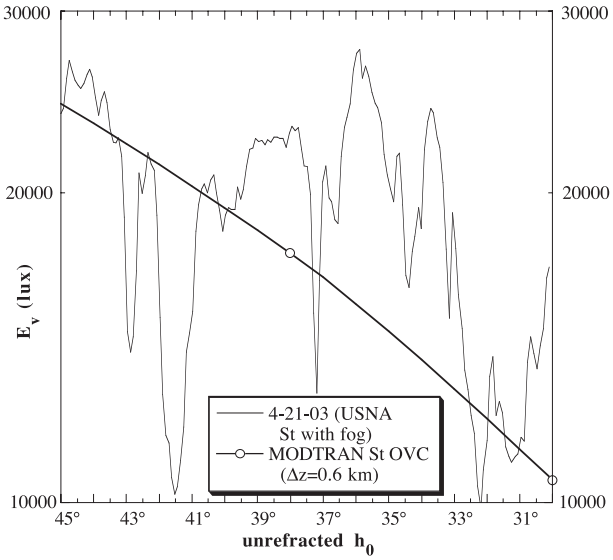

Fig. 14. Comparison of horizontal illuminance $E_v(h_0)$ simulated by radiative transfer model MODTRAN4 and measured at USNA on 4-21-03. The USNA E_v time series is unusually noisy, apparently because of persistent thick fog (horizontal visibility distance ~0.5–1 km) between the surface and the intermittently visible cloud base.

case). Once again, angular or spatial variability in cloud τ better seems to explain our measured E_v fluctuations.

In fact, Fig. 13 gives two spectacular examples of how twilight E_v variability depends on cloud τ. In the 10-10-99 Marion Center case, moderate to dense fog continually enveloped the observing site, and pronounced E_v fluctuations persisted throughout twilight. Note that fog is associated once again with an unusually variable E_v time series (see also Figs. 9, 11, and 14).

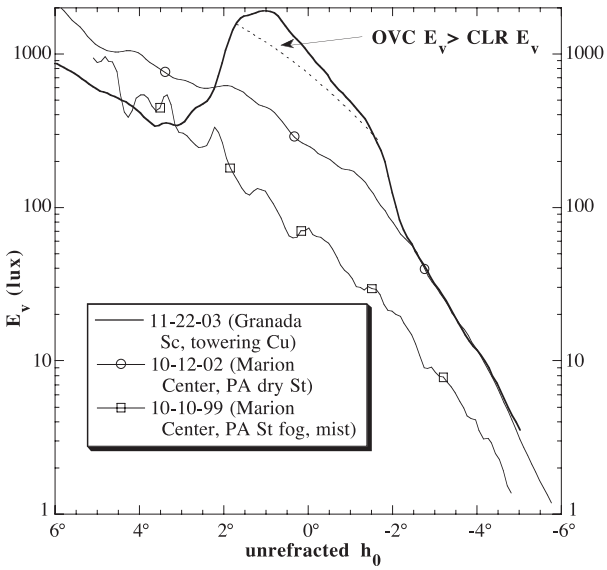

Fig. 13. Horizontal illuminance E_v as a function of h_0 before and during three overcast twilights at Granada, Spain (11-22-03) and at Marion Center (10-12-02 and 10-10-99). Near sunset at Granada, towering cumulus diffusely reflected enough direct and diffuse sunlight through the overcast to briefly make its E_v exceed those of a typical clear sky at the same h_0 (dashed curve).

Another extreme is Fig. 13's Granada overcast of 11-22-03. Near sunset, this overcast thinned enough to let towering cumulus (Cu) diffusely reflect large amounts of direct, reddened sunlight to the surface. As a result, the still-intact overcast was briefly brighter than a clear sky at the same h_0 (dashed curve; $t_{el} \sim 18.5$ min). This is the important exception noted above to the truism that overcasts are always darker than clear skies. In our experience, such brightening is both rare and visually remarkable: it occurs only when tall clouds top the overcast, and it is one of the few cases when overcast E_v fluctuations prompt glances skyward.

At present, we cannot model this complex range of overcast variability very realistically. For example, Fig. 14 compares a highly variable stratus overcast at USNA on 4-21-03 with the E_v trend predicted by the radiative transfer model MODTRAN4. Despite MODTRAN's complexity and versatility, its verisimilitude is not striking in Fig. 14 for fixed model cloud thickness Δz. Figure 14's MODTRAN simulation parameters include typical seasonal atmospheric profiles of temperature, pressure, humidity, and gas mixing ratios at midlatitudes; a default stratus cloud model from z = 330–930 m; tropospheric aerosols typical of rural sites; background stratospheric dust and other aerosols; Mie aerosol phase functions; multiple scattering; and an underlying Lambertian surface with reflectance = 0.2. Changing any one of these parameters does not reproduce Fig. 14's observed E_v trend.

Although we could match this trend by continually varying MODTRAN Δz, the exercise would be purely

ad hoc without having detailed knowledge of actual cloud Δz. In fact, MODTRAN makes a fairly common modeling assumption: the atmosphere is horizontally homogeneous. Changing a MODTRAN atmosphere's fixed Δz over time or h_0 is easy, but adding the radiative-transfer consequences of overcasts' horizontal inhomogeneity will require new modeling tracks,[4–8] perhaps including the use of fractal clouds.[18]

6. Conclusions

Although temporal variability of overcast E_v tends to increase with decreasing cloud τ, counterexamples are easy to find (e.g., Figs. 7, 9). Twilight h_0, subcloud snowfall, and stratus or stratocumulus cloud type also have mixed effects on E_v noisiness, if indeed such cause-and-effect relationships exist. Brightness variability increases more consistently for (1) fog or near-surface stratus, (2) clouds that have more visual detail, and (3) narrower instrument FOV (i.e., L_v versus E_v). Time-lapse photography of overcasts reveals that their mid- to high-frequency L_v and E_v fluctuations (say, $\Delta t < 10$–15 min) often are dominated by cloud elements of different τ that move across the radiometer FOV, not by τ changes within individual clouds. However, lower-frequency changes in mean overcast τ also appear to contribute to the observed overcast variability (e.g., Figs. 3, 4, and 11).

The practical significance of short-term fluctuations in overcast luminance and illuminance is as yet unknown. However, being aware of their existence and knowing how to describe their full range clearly is necessary in developing realistic overcast models. The limitations of even so sophisticated a model as MODTRAN4 (Fig. 14) illustrate the large gap between our ability to observe and to predict overcast L_v or E_v. As we have shown above, temporal frequency analyses such as the SDF are useful tools for quantifying overcast variability and for vetting the time- and space-dependent details of new models of overcast brightness.

Several agencies generously funded this research. Lee was supported by the United States National Science Foundation grant ATM-0207516 and by the United States Naval Academy's Departments of Physics and Mathematics. Hernández-Andrés was supported by Spain's Comisión Interministerial de Ciencia y Tecnología (CICYT) under research grant DPI2004-03734.

References and Notes

1. R. L. Lee, Jr. and J. Hernández-Andrés, "Colors of the daytime overcast sky," Appl. Opt. **44,** 5712–5722 (2005).
2. J. A. Love, "Determination of the daylight factor under real overcast skies," J. Illum. Eng. Soc. **22,** 176–182 (1993).
3. J. A. Lynes, *Principles of Natural Lighting* (Elsevier, Amsterdam, 1968), p. 77.
4. R. Terra, C. R. Mechoso, and A. Arakawa, "Impact of orographically induced spatial variability in PBL stratiform clouds on climate simulations," J. Climate **17,** 276–293 (2004).
5. H. W. Barker, G. L. Stephens, P. T. Partain, J. W. Bergman, B. Bonnel, K. Campana, E. E. Clothiaux, S. Clough, S. Cusack, J. Delamere, J. Edwards, K. F. Evans, Y. Fouquart, S. Freidenreich, V. Galin, Y. Hou, S. Kato, J. Li, E. Mlawer, J.-J. Morcrette, W. O'Hirok, P. Räisänen, V. Ramaswamy, B. Ritter, E. Rozanov, M. Schlesinger, K. Shibata, P. Sporyshev, Z. Sun, M. Wendisch, N. Wood, and F. Yang, "Assessing 1D atmospheric solar radiative transfer models: interpretation and handling of unresolved clouds," J. Climate **16,** 2676–2699 (2003).
6. M. Sengupta, E. E. Clothiaux, T. P. Ackerman, S. Kato, and Q. Min, "Importance of accurate liquid water path for estimation of solar radiation in warm boundary layer clouds: an observational study," J. Climate **16,** 2997–3009 (2003).
7. A. B. Davis and A. Marshak, "Space–time characteristics of light transmitted through dense clouds: a Green's function analysis," J. Atmos. Sci. **59,** 2713–2727 (2002).
8. M. Szczodrak, P. H. Austin, and P. B. Krummel, "Variability of optical depth and effective radius in marine stratocumulus clouds," J. Atmos. Sci. **58,** 2912–2926 (2001).
9. J. J. Delaunay, M. Rommel, and J. Geisler, "The importance of the sampling frequency in determining short-time-averaged irradiance and illuminance for rapidly changing cloud cover," Solar Energy **52,** 541–545 (1994).
10. See Ref. 1, Sect. 2 for details of our overcast definition. Here we use "brightness" as a shorthand for the photometric measures of illuminance and luminance, while recognizing that brightness has several psychophysical definitions, including those that relate it quantitatively to luminance. For details, see G. Wyszecki and W. S. Stiles, *Color Science: Concepts and Methods, Quantitative Data and Formulae*, 2nd ed. (Wiley, New York, 1982), pp. 493–494.
11. D. R. E. Brown, *Natural Illumination Charts*, Report #374-1 (U.S. Navy Bureau of Ships, Washington, DC, 1952).
12. C. F. Bohren, "Multiple scattering of light and some of its observable consequences," Am. J. Phys. **55,** 524–533 (1987).
13. For Fig. 3's 10-17-03 E_v curve, $P_6 = -5.289 \times 10^7 + 1.051 \times 10^7 h_0 - 7.829 \times 10^5 h_0^2 + 24660 h_0^3 - 135.6 h_0^4 - 9.044 h_0^5 + 0.1459 h_0^6$ for h_0 in degrees. The units of P_6 are lux, and its curvilinear correlation coefficient is 0.9734 for the 10-17-03 time series.
14. D. B. Percival and A. T. Walden, *Spectral Analysis for Physical Applications: Multitaper and Conventional Univariate Techniques* (Cambridge University, Cambridge, UK, 1993), pp. 127–144, 196–215.
15. Although the h_0 interval is the same for Fig. 4's SDF curves, their t_{el} differ and thus so do the maximum periods (and minimum frequencies) graphed in Fig. 4.
16. Research on the angular, as opposed to temporal, relationship between overcast L_v and E_v is both extensive and long-lived. An important early study is S. Fritz, "Illuminance and luminance under overcast skies," J. Opt. Soc. Am. **45,** 820–825 (1955).
17. We distinguish between fog and a higher-altitude overcast only when the two cloud types' movement and structure clearly differ. For our ground-based observations, this distinction requires that the fog occasionally thins enough to let us see the overcast above it. For the canonical definition of fog, see T. S. Glickman, ed., *Glossary of Meteorology*, 2nd ed. (American Meteorological Society, Boston, 2000), pp. 304–305.
18. C. Kuchinke, K. Fienberg, and M. Nunez, "The angular distribution of UV-B sky radiance under cloudy conditions: a comparison of measurements and radiative transfer calculations using a fractal cloud model," J. Appl. Meteorol. **43,** 751–761 (2004).